Algorithms and Viewsheds for Terrain Assessment

Ankush Acharyya, Ramesh K. Jallu
The Czech Academy of Sciences
Institute of Computer Science, Prague, Czech Republic

Maarten Löffler
Deptartment of Information and Computing Sciences
Utrecht University, The Netherlands

Gert G.T. Meijer
Academy of ICT and Creative Technologies
NHL Stenden University of Applied Sciences
The Netherlands

Maria Saumell
The Czech Academy of Sciences, Institute of Computer Science, Prague, Czech Republic
Department of Theoretical Computer Science
Faculty of Information Technology
Czech Technical University in Prague, Czech Republic

Rodrigo I. Silveira
Department of Mathematics, Universitat Politècnica de Catalunya
Barcelona, Spain

Frank Staals
Department of Information and Computing Sciences
Utrecht University
The Netherlands

ABSTRACT: *In this work, we use the computing view sheds for terrain analysis. The viewshed's characteristics may change based on the nature of terrain and the position of the viewpoint. We addressed a new topographic feature, the prickliness, that measures the number of local maxima in a terrain from all possible angles of view. During the evaluation we observed that the prickliness effectively captures the potential of terrains to have high complexity viewsheds. To do the statistical analysis, we prepared and published near-optimal algorithms to compute it for TIN terrains, and efficient approximate algorithms for raster DEMs. During the experimentation process, we found the validation of the usefulness of the prickliness attribute with experiments.*

Keywords: Digital Elevation Model, Triangulated Irregular Network, Viewshed Complexity

Received: 8 April 2021, Revised 17 July 2021, Accepted 22 July 2021

DOI: 10.6025/jism/2021/11/4/103-116

1. Introduction

Digital terrain models represent part of the earth's surface, and are used to solve a variety of problems in geographic ç science. An important task is viewshed analysis: determining which parts of a terrain are visible from certain terrain locations. Two points p and q are mutually *visible* if the line of sight defined by line segment $\overline{pq}$ does not intersect the interior of the terrain. Given a *viewpoint* p, the *viewshed* of p is the set of all terrain points that are visible from p. Similarly, the viewshed of a set of viewpoints P is defined as the set of all terrain points that are visible from *at least* one viewpoint in P. Viewsheds are useful, for example, in evaluating the visual impact of potential constructions [2], analyzing the coverage of an area by fire watchtowers [12], or measuring the scenic beauty of a landscape [1, 21].

Discrete and Continuous Terrain Representations. Two major terrain representations are prevalent in GIS. The simplest and most widespread is the raster, or *digital elevation model* (DEM), consisting of a rectangular grid where each cell stores an elevation.[①] The main alternative is a vector representation, or *triangulated irregular network* (TIN), where a set of irregularly spaced elevation points are connected into a triangulation. A TIN can be viewed as a continuous xy-monotone polyhedral surface in $\mathbb{R}^3$. A viewshed in a DEM is the set of all raster cells that are visible from at least one viewpoint. In contrast, a viewshed in a TIN is the union of all parts of triangles that are visible from at least one viewpoint.

DEMs are simpler to analyze than TINs and facilitate most analysis tasks. The main advantage of TINs is that they require less storage space. Both models have been considered extensively in the literature for viewshed analysis, see Dean [4] for a complete comparison of both models in the context of forest viewshed. Some studies suggest that TINs can be superior to DEMs in viewshed computations [4], but experimental evidence is inconclusive [19]. This is in part due to the fact that the viewshed algorithms used in [19] do not compute the visible part of each triangle, but only attempt to determine whether each triangle is completely visible. This introduces an additional source of error and does not make use of all the information contained in the TIN.

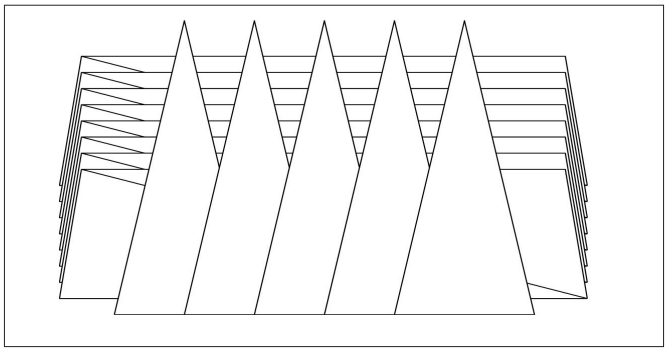

Figure 1. Part of a TIN with a high-complexity viewshed. The viewpoint (not shown) is placed at the center of projection. The relevant triangles of the TIN are the ones shown, which define n peaks and ridges. The viewshed in this case is formed by $\Theta(n^2)$ visible regions

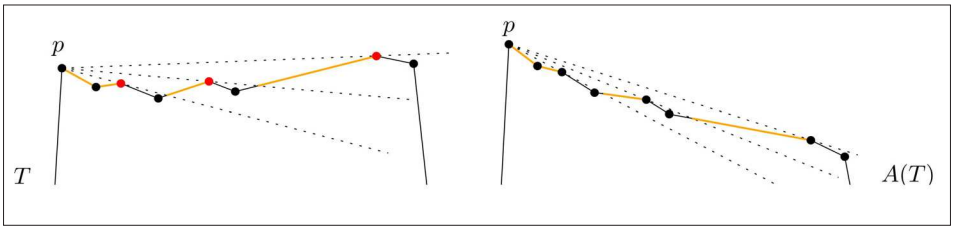

Figure 2. Left: a TIN (1.5D profile) with three peaks and one viewpoint (p), with a viewshed composed of three parts (visible parts shown orange). Right: transformation of the terrain with no peaks (other than p) but the same viewshed complexity. Dotted segments show lines of sight from p

[①] For the sake of simplicity, in this paper we use DEM to denote the raster version of a DEM.

Viewshed Complexity. The algorithmic study of viewsheds focuses on two main aspects: the complexity of the viewsheds, and their efficient computation. In this work, we are interested in their complexity. We use the information-theoretic meaning of "complexity": the complexity of an object is the number of bits needed to represent it in memory. Therefore, in the case of TINs, viewshed complexity is defined as the total number of vertices of the polygons that form the viewshed. In the case of DEMs, there are several ways to measure viewshed complexity. To facilitate comparison between TIN and DEM viewsheds, we convert the visible areas in the raster viewshed to polygons, and define the viewshed complexity as the total number of vertices in those polygons. A typical high-complexity viewshed construction for a TIN is shown schematically in Figure 1, where one viewpoint would be placed at the center of projection, and both the number of vertical and horizontal triangles is $\Theta(n)$, for n terrain vertices. The vertical peaks form a grid-like pattern with the horizontal triangles, leading to a viewshed with $\Theta(n^2)$ visible triangle pieces.

While a viewshed can have high complexity, this is expected to be uncommon in real terrains [3]. There have been attempts to define theoretical conditions for a (TIN) terrain that guarantee, among others, that viewsheds cannot be that large. For instance, Moet et al. [18] showed that if terrain triangles satisfy certain "realistic" shape conditions, viewsheds have $O(n\sqrt{n})$ complexity. De Berg et al. [3] showed that similar conditions guarantee worst-case expected complexity of $\Theta(n)$ when the vertex heights are subject to uniform noise.

Viewsheds and Peaks. The topography of the terrain has a strong influence on the potential complexity of the viewshed. To give an extreme example, in a totally concave terrain, the viewshed of any viewpoint will be the whole terrain, and has a trivial description. Intuitively, to obtain a high complexity viewshed as in Figure 1, one needs a large number of obstacles obstructing the visibility from the viewpoint, which requires a somewhat rough topography.

In fact, it is well-established that viewsheds tend to be more complex in terrains that are more "rugged" [13]. This leads to the natural question of which terrain characteristics correlate with high complexity viewsheds. Several topographic attributes have been proposed to capture different aspects of the roughness of a terrain, such as the *terrain ruggedness index* [20], the *terrain shape index* [16], or the *fractal dimension* [14]. These attributes focus on aspects like the amount of elevation change between adjacent parts of a terrain, its overall shape, or the terrain complexity. However, none of them is specifically intended to capture the possibility to produce high complexity viewsheds, and there is no theoretical evidence for such a correlation. Moreover, these attributes are locally defined, and measure only attributes of the local neighborhood of one single point. While we can average these measures over the whole terrain, given the global nature of visibility, it is unclear a priori whether such measures are suitable for predicting viewshed complexity. We refer to Dong et al. [5] for a systematic classification of topographic attributes.

One very simple and natural global measure of the ruggedness of a terrain that is relevant for viewshed complexity is to simply count the number of *peaks* (i.e., local maxima) in the terrain. It has been observed in the literature that areas with higher elevation difference, and hence, more peaks, cause irregularities in viewsheds [9, 12], and this idea aligns with our theoretical understanding: the quadratic example from Figure 1 is designed by creating an artificial row of peaks, and placing a viewpoint behind them. However, while it seems reasonable to use the peak count as complexity measure, there is no theoretical correlation between the number of peaks and the viewshed complexity. This is easily seen by performing a simple trick: any terrain can be made arbitrarily flat by scaling it in the z-dimension by a very small factor, and then rotating it slightly – this results in a valid terrain without any peaks, but retains the same viewshed complexity. See Figure 2 for an example in 1.5D. In fact, viewshed complexity is invariant under affine transformations (i.e., scalings, rotations, and translations) of the terrain: the application of any affine combination to the terrain and the viewpoints results in a viewshed of the same complexity. Hence, any measure that has provable correlation with it must be affine-invariant as well. This is a common problem to establish theoretical guarantees on viewshed complexity, or to design features of "realistic" terrains in general [3, 18]. In fact, it is easy to see that none of the terrain attributes mentioned above is affine-invariant.

Prickliness. In this work we propose a new topographic attribute: the *prickliness*. The definition follows directly from the above observations: it counts the number of peaks in a terrain, but does so *for every possible affine transformation* of the terrain. We first present a definition for TINs, and then we explain how the definition carries over to DEMs.

Let T be a triangulated surface that is xy-monotone. Let A be an affine transformation, and let $A(T)$ be the terrain obtained after applying A to T. We define $m(A(T))$ to be the number of internal and convex vertices of $T^{②}$ that are peaks in $A(T)$. Let

$A(T)$ be the set of all affine transformations of T. We define the *prickliness* of T, $\pi(T)$, to be the maximum number of local maxima over all transformations of T; that is, $\pi(T) = max_{A \in A(T)} m(A(T))$. We start by observing that, essentially, the prickliness considers all possible *directions* in which the number of peaks are counted. Let $\vec{v}$ be a vector in $\mathbb{R}^3$. Let $\pi_{\vec{v}}(T)$ be the number of internal and convex vertices of T that are local maxima of T in direction $\vec{v}$; that is, the number of internal and convex vertices of T for which the local neighborhood does not extend further than that vertex in direction $\vec{v}$.

Observation 1. $\pi(T) = \max_{\vec{v}} \pi_{\vec{v}}(T)$

Using this observation, we reduce the space of all affine transformations to the 2- dimensional space of all directions in 3D. Since T is a terrain, for any $\vec{v}$ with a negative z-coordinate we have $\pi_{\vec{v}}(T) = 0$ by definition, thus the interesting directions reduce to the points on the (positive) unit half-sphere. This provides a natural way to visualize the prickliness of a terrain. Each direction can be expressed using two angles θ and ϕ (i.e., using spherical coordinates), where θ represents the polar angle and ϕ the azimuthal angle. Figure 3 shows a small terrain and the resulting prickliness, showing a projection of the half-sphere, where each point represents a direction, and its color indicates its prickliness. Note that we specifically define prickliness to be the *maximum* over all orientations rather, say, the average over all orientations. Even for a terrain with high-complexity viewsheds like the one in Figure 1, the average number of peaks would still be relatively small since there are many orientations with a small number of peaks. Hence, such a definition is unlikely to accurately capture the complexity of viewsheds on a terrain.

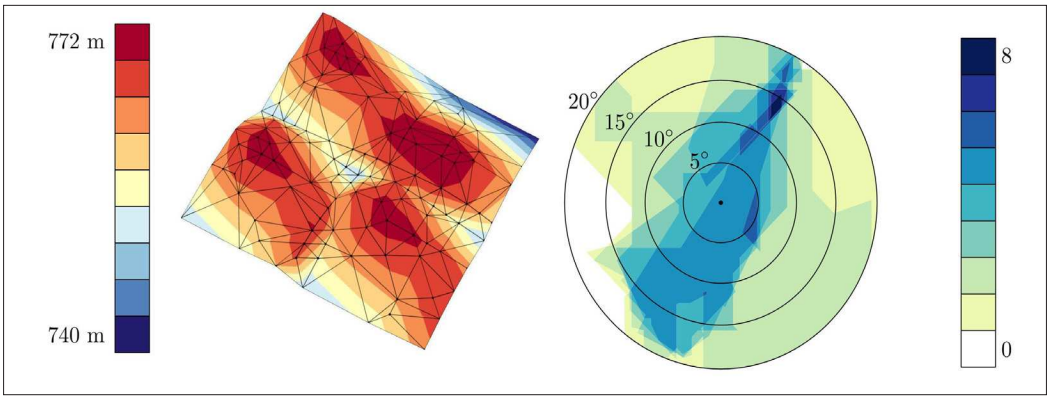

Figure 3. (left) A TIN T, with triangulation edges shown in black, and elevation indicated using colors. (right) A visualization of the prickliness of T as a function of the angles (θ, ϕ) that define each direction (circles indicate contour lines for); color indicates prickliness. The maximum prickliness is 8, attained at a direction of roughly $\theta = 13^o$ and $\phi = 60^o$ (north-east from the origin)

We notice that all previous notions easily translate to DEMs. The centers of the DEM cells can be seen as the *vertices* of the terrain, and every internal vertex of the terrain has eight neighbors given by the cell centers of the eight neighboring cells. Hence, in the definitions for DEMs, the notion of *adjacent vertices* for TINs is replaced by that of *neighbors*. A vertex is a local maximum for some affine transformation of the terrain if all of its neighbors have a lower or equal z-coordinate. This gives an equivalent definition of $\pi(T)$ when T is a DEM.

Results and organization. The remainder of this paper is organized as follows.

In Section 2, we review existing topographic attributes in more detail, and discuss how attributes defined for DEMs can be adapted to TINs.

We show in Section 3 that the viewshed complexity of a single viewpoint in a TIN terrain cannot be higher than $O(n \cdot \pi(T))$, and this is tight.

In Section 4, we consider the question of how to compute prickliness. We provide an $O(n^2)$ time algorithm for TIN terrains,

which is near-optimal, and an efficient approximate algorithm for DEM terrains.

In Sections 5-7, we report on experiments that measure the values of distinct topographic attributes (including the prickliness) of real terrains, and analyze their possible correlation with viewshed complexity. From the experiments, we conclude that prickliness provides such a correlation in the case of TIN terrains, while the other measures perform more poorly. The situation for DEM terrains is less clear.

Finally, we provide our code implementing two key algorithms for this work: an algorithm to calculate the prickliness of a TIN terrain and an algorithm to calculate the combined viewshed originating from a set of multiple viewpoints.

2. Topographic Attributes

In addition to prickliness, we consider the following topographic attributes, and their relation to viewshed complexity.

Terrain Ruggedness Index (TRI). The Terrain Ruggedness Index measures the variability in the elevation of the terrain [20]. Riley et al. originally defined TRI specifically for DEM terrains as follows. Let c be a cell of the terrain, and let $\mathcal{N}(c)$ denote the set of (at most) eight neighboring cells of c. The TRI of c is then defined as

$$pTRI(c) = \sqrt{\frac{1}{|\mathcal{N}(c)|} \sum_{q \in \mathcal{N}(c)} (c_z - q_z)^2},$$

where $|\mathcal{N}(c)|$ denotes the cardinality of $\mathcal{N}(c)$. Hence, *pTRI* (*c*) essentially measures the standard deviation of the difference in height between c and the points in N(c). The Terrain Roughness Index *TRI* (*T*) of *T* is the average *pTRI* (*T, c*) value over all cells c in T.

For TINs, we have adapted the definition as follows: $\mathcal{N}(c)$ is defined as the set of vertices which are adjacent to a given vertex c in T. The Terrain Roughness Index *TRI* (*T*) is then obtained as the average *pTRI* (*T, c*) value over all vertices c of T.

Terrain Shape Index (TSI). The Terrain Shape Index also measures the "shape" of the terrain [16]. Let *C* (*c, r, T*) denote the intersection of *T* with a vertical cylinder of radius r centered at c (so after projecting all points to the plane, the points in *C*(*c, r, T*) lie on a circle of radius r centered at c). For ease of computation, we discretize *C* (*c, r, T*): for DEMs we define *C*(*c, r, T*) to be the grid cells intersected by *C* (*c, r, T*), and for TINs we define *C* (*c, r, T*) as a set of 360 equally spaced points on C(*c, r, T*). The TSI of a point c is then defined as

$$pTSI(c, r, T) = \frac{1}{r|C(c, r, T)|} \sum_{q \in C(c,r,T)} c_z - q_z \ ,$$

and essentially measures the average difference in height between "center" point c and the points at (planar) distance r to c, normalized by r. The Terrain Shape Index *TSI* (*T, r*) of the entire terrain *T* is the average *pTSI* (*c, r, T*) over all cells (in case of a DEM) or vertices (in case of a TIN) of T. We choose r = 1000m (which is roughly eight percent of the width of our terrains) in our experiments.

Fractal Dimension (FD). The (local) fractal dimension measures the roughness around a point c on the terrain over various scales [14, 22]. We use the definition of Taud and Parrot [22] that uses a box-counting method, and is defined as follows. Let w be the width of a cell in the DEM, and let $s \in \mathbb{N}$ be a size parameter. For $q \in 1..s/2$, consider subdividing the cube with side length sw centered at c into $(s/q)^3$ cubes of side length qw. Let $C_s(c, q)$ denote the resulting set of cubes, and define $N_s(c, q, T)$ as the number of cubes from $C_s(c, q)$ that contain a "unit" cube from $C_s(c, 1)$ lying fully below the terrain T. Let $l_s(c, T)$ be the linear function that best fits (i.e. minimizes the sum of squared errors) the set of points $\{(\ln(q), \ln(N_s(c, q, T))) \mid q \in 1..s/2\}$ resulting from those measurements. The fractal dimension $pFD_s(c, T)$ at c is then defined as the inverse of the slope of $l_s(c, T)$. The fractal dimension $FD(T, s)$ of the DEM terrain itself is again the average over all DEM cells. Following Taud and

Parrot we use $s = 24$ in our experiments. For our TIN terrains, we keep w the same as in their original DEM representations, and average over all vertices.

3. Prickliness and Viewshed Complexities

In this section we show that there is a provable relation between prickliness and viewshed complexity. We present our analysis for TINs, since they provide a natural way to measure viewshed complexity. However, a similar analysis can be carried out for DEMs as well.

Let v be a vertex of T, and let p be a viewpoint. We denote by $\uparrow_p^v$ the half-line with origin at p in the direction of vector $\overrightarrow{pv}$. Now, let $e = uv$ be an edge of T. The *vase* of p and e, denoted $\uparrow_p^e$, is the region bounded by e, $\uparrow_p^u$, and $\uparrow_p^v$ (see Figure 4).

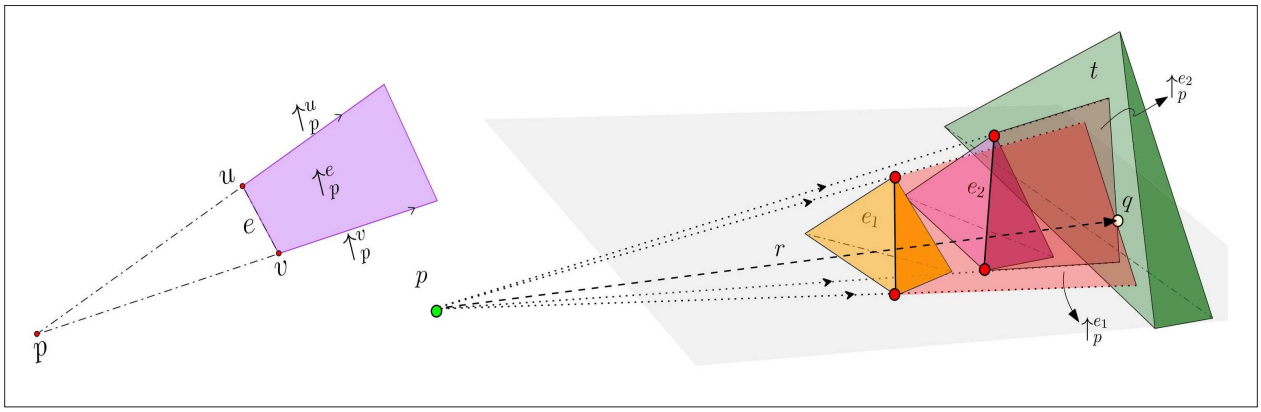

Figure 4. A vase

Figure 5. The situation in the proof of Lemma 3

Vertices of the viewshed of p can have three types [11]. A vertex of type 1 is a vertex of T, of which there are clearly only n. A vertex of type 2 is the intersection of an edge of T and a vase. A vertex of type 3 is the intersection of a triangle of T and two vases.

Lemma 2. *There are at most* $O(n \cdot \pi(T))$ *vertices of type* 2.

Proof. Consider an edge e of T and let H be the plane spanned by e and p. Consider the viewshed of p on e. Let qr be a maximal invisible portion of e surrounded by two visible ones. Since q and r are vertices of type 2, the open segments pq and pr pass through a point of T. On the other hand, for any point x in the open segment qr, there exist points of T above the segment px. This implies that there is a continuous portion of T above H such that the vertical projection onto H of this portion lies on the triangle pqr. Such portion has a local maximum in the direction perpendicular to H which is a convex and internal vertex of T. In consequence, each invisible portion of e surrounded by two visible ones can be assigned to a distinct point of T that is a local maximum in the direction perpendicular to H. Hence, in the viewshed of p, e is partitioned into at most $2\pi(T) + 3$ parts.

Lemma 3. *There are at most* $O(n \cdot \pi(T))$ *vertices of type* 3.

Proof. Let q be a vertex of type 3 in the viewshed of p. Point q is the intersection between a triangle t of T and two vases, say, $\uparrow_p^{e_1}$ and $\uparrow_p^{e_2}$; see Figure 5. Let r be the ray with origin at p and passing through q. Ray r intersects edges e_1 and e_2. First, we suppose that e_1 and e_2 do not share any vertices and, without loss of generality, we assume that $r \cap e_1$ is closer to p than $r \cap e_2$. Notice that $r \cap e_2$ is a vertex of type 2 because it is the intersection of e_2 and $\uparrow_p^{e_1}$, and $\uparrow_p^{e_1}$ partitions e_2 into a visible and an invisible portion. Thus, we charge q to $r \cap e_2$. If another vertex of type 3 was charged to $r \cap e_2$, then such a vertex would also lie on r. However, no point on r after q is visible from p because the visibility is blocked by t. Hence, no other vertex of type 3 is charged to $r \cap e_2$.

If e_1 and e_2 are both incident to a vertex v, since $t \cap \uparrow_p^{e1} \cap \uparrow_p^{e2}$ is a type 3 vertex, we have that r passes through v. Therefore, q is the first intersection point between r (which can be seen as the ray with origin at p and passing through v) and the interior of some triangle in T. Therefore, any vertex v of T creates at most a unique vertex of type 3 in this way.

Theorem 4. Let T be a *TIN* terrain with n vertices and prickliness $\pi(T)$. The complexity of a viewshed is $O(n \cdot \pi(T))$. This bound is asymptotically tight.

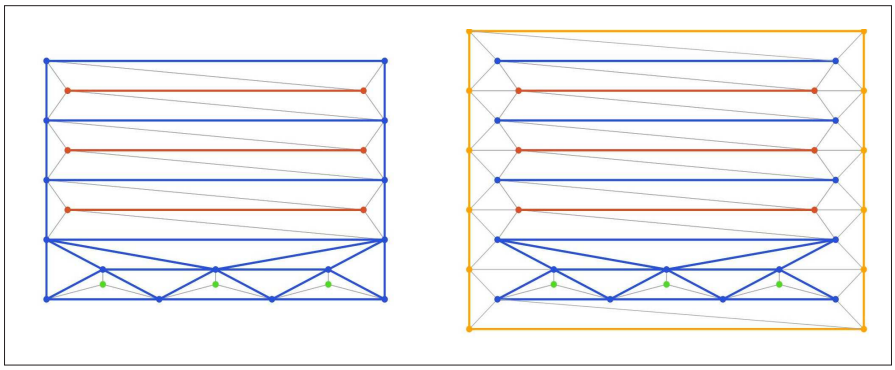

Figure 6. Schematic top-down view of the classic quadratic construction (left), and the same adapted to have small rickliness (right). If an observer is at $(0, -\infty)$, the resulting view has quadratic complexity (see Figure 1). Blue vertices/ edges are low, red are medium height, and green are high. The right construction introduces a new height (yellow) between medium and high, and changes the triangulation slightly, to ensure that all convex vertices in the construction are green.

Proof. The upper bound on the complexity follows directly from Lemmas 2 and 3. Hence, we focus on the lower bound; i.e. we show that there exists a terrain T with prickliness $\pi(T)$, and a viewpoint on T with viewshed whose complexity is $\Omega(n \cdot \pi(T))$.

Consider the standard quadratic viewshed construction, composed of a set of front mountains and back triangles (Figure 6 (left)). Notice that there can be at most $\pi(T)$ mountains "at the front". We add a surrounding box around the construction, see Figure 6 (right), such that each vertex of the back triangles is connected to at least one vertex on this box. We set the elevation of the box so that it is higher than all the vertices of the back triangles, but lower than those of the front mountains. In this way, no vertex of the back triangles will be a local maximum in any direction, and all local maxima will come from the front.

4. Prickliness Computation

4.1. Algorithm for TINs

For every convex terrain vertex v, we compute the region of the unit sphere $\mathbb{S}^2$ containing all vectors $\vec{w}$ such that v is a local maximum of T in direction $\vec{w}$. As we will see, such a region is a cone and we denote it by $co(v)$. To compute $co(v)$, we consider all edges of T incident to v. Let $e = vu$ be such an edge, and consider the plane orthogonal to e through v. Let H be the half-space which is bounded by this plane and does not contain u. We translate H so that the plane bounding it contains the origin; let H_e be the intersection of the obtained half-space with the unit sphere $\mathbb{S}^2$. The following property holds: For any unit vector $\vec{w}$ in H_e, the edge e does not extend further than v in direction $\vec{w}$. We repeat this procedure for all edges incident to v, and consider the intersection $co(v)$ of all the obtained half-spheres H_e. For any unit vector $\vec{w}$ in $co(v)$, none of the edges incident to v extends further than v in direction $\vec{w}$. Since v is convex, this implies that v is a local maximum in direction $\vec{w}$.

Once we know all regions of type $co(v)$, computing the prickliness of T reduces to finding unit vector that lies in the maximum number of such regions. To simplify, rather than considering these cones on the sphere, we extend them until they intersect the boundary of a unit cube $\mathbb{Q}$ centered at the origin. The conic regions of type $co(v)$ intersect the faces of $\mathbb{Q}$ forming (overlapping) convex regions. Notice that the problem of finding a unit vector that lies in the maximum number of regions of type $co(v)$ on $\mathbb{S}$ is equivalent to the problem of finding a point on the surface of $\mathbb{Q}$ that lies in the maximum number of "extended" regions of type $co(v)$. The second problem can be solved by computing the maximum overlap of

convex regions using a topological sweep [6], for each face of the cube.

Computing the intersection between the extended regions of type $co(v)$ (for all convex vertices v) and the boundary of $\mathbb{Q}$ takes $O(n \log n)$ time, and topological sweep to find the maximum overlap takes $O(n^2)$ time. We obtain the following:

Theorem 5. *The prickliness of an n-vertex TIN terrain can be computed in* $O(n^2)$ *time.*

4.2. Algorithm for DEMs

The prickliness of a DEM terrain can be computed using the same algorithm as for TINs: Each cell center can be seen as a vertex v, and its neighbors are the cell centers of its eight neighboring cells. The edges connecting v to its neighbors can then be used to compute $co(v)$ as in Section 4.1, and the rest of the algorithm follows. However, DEM terrains have significantly more vertices, and vertices have on average more neighbors; this causes a significant increase in computation time and, more importantly, in memory usage. For this reason, in our experiments, the prickliness values for the DEM terrains were approximated.

The approximated algorithm discretizes the set of vectors that are candidates to achieve prickliness as follows: For every interior cell g of the terrain, we translate a horizontal grid G of size n by n and cell size s above the cell center v of g in a way that v and the center of G are vertically aligned and at distance one. Then the vectors considered as potential prickliness are those with origin at v and endpoint at some cell center c in G. For any such vector lying inside $co(v)$, the value of c gets incremented by one. When all interior cells of the terrain have been processed, a cell center of G with maximum value gives the approximated prickliness of the terrain. Cell size s was set to 0.05, based on the spread of the results on TIN terrains. This method should, in practice, produce a close approximation of prickliness.

5. Experiments

In this section we present our experimental setup. Our goals are to

- Verify our hypothesis that existing topographic attributes do not provide a good indicator of the viewshed complexity,
- Evaluate whether prickliness *does* provide a good indicator of viewshed complexity in practice, and
- Evaluate whether these results are consistent for DEMs and TINs.

Furthermore, since in many applications we care about the visibility of multiple viewpoints (e.g. placing guards or watchtowers), we also investigate these questions with respect to the complexity of the common viewshed of a set of viewpoints. In this setting a point is part of the (common) viewshed if and only if it can be seen by at least one viewpoint. Note that since Theorem 4 *proves* that the complexity of a viewshed is proportional to the prickliness, our second goal is mainly to evaluate the practicality of prickliness. That is, to establish if this relation is also observable in practice or that the hidden constants in the big-O notation are sufficiently large that the relation is visible only for very large terrains.

Next, we briefly describe our implementations of the topographic attributes. We then outline some basic information about the terrain data that we use as input, and we describe how we select the viewpoints for which we compute the viewsheds.

Implementations. We consider prickliness and the topographic attributes from Section 2. To compute the prickliness we implemented the algorithm from Theorem 4 in C++ using CGAL 5.0.2 [23] and its *2D arrangements* [24] library[③]. We also implemented the algorithms for TRI, TSI, and FD on TINs. These are mostly straightforward. To compute the viewsheds on TINs we implemented the hidden-surface elimination algorithm of [10] using CGAL.c$ We remark that our implementation computes the exact TIN viewsheds, as opposed to previous studies that only considered fully visible triangles (e.g., [19]).

To compute the prickliness on DEMs we used the algorithm from Section 4.2. For TRI, TSI, and FD on DEMs we used the implementations available in ArcGIS Pro 2.5.1 [7]. To compute viewsheds on DEMs we used the builtin tool "Viewshed 2" in

[③] Source code available from https://github.com/GTMeijer/Prickliness.

rcGIS, which produces a raster with boolean values that indicate if a cell is visible or not. To get a measure of complexity similar to that of the TINs we use the "Raster to Polygon" functionality of ArcGIS (with its default settings) to convert the set of True cells into a set of planar polygons (possibly with holes). We use the total number of vertices of these polygons as the complexity of the viewshed on a DEM.

Terrains. We considered a collection of 52 real-world terrains around the world. These terrains were handpicked in order to cover a large variety of landscapes, with varying ruggedness, including mountainous regions (Rocky mountains, Himalaya), lat areas (farmlands in the Netherlands), and rolling hills (Sahara), and different complexity. We obtained the terrains through the *Terrain* world elevation layer [8] in ArcGIS [7]. Each terrain is represented as a 10-meter resolution DEM of size 1400×1200. According to past studies the chosen resolution of 10 meters provides the best compromise between high resolution and processing time of measurements [15, 25]. The complete list of terrains with their extents can be found in [17].

We generated a TIN terrain for each DEM using the *"Raster to TIN"* function in ArcGIS [7]. This function generates a Delaunay triangulation to avoid long, thin triangles as much as possible. With the *z-tolerance* setting, the triangulation complexity can be controlled by determining an allowed deviation from the DEM elevation values. We considered TIN terrains generated using a *z*-tolerance of 50 meters. This resulted in TINs where the number of vertices varied between 30 and 5808 (with an average of 1547 vertices). Their distribution can be seen in Figure 8.

Viewpoints. Kim et al. [13] found that placing the viewpoints at peaks typically produces viewsheds that cover hilltops, but not many valleys, whereas placing viewpoints in pits typically covers valleys but not hilltops. This leads us to consider three different strategies to pick the locations of the viewpoints: picking "high" points (to cover peaks), picking "low" points (to

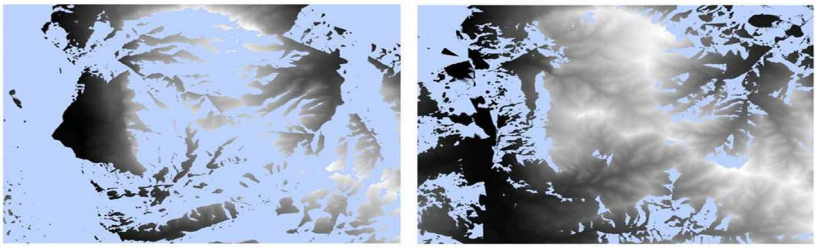

Figure 7. (left) A joint viewshed (blue) created from viewpoints placed on the highest points. (right) A joint viewshed (blue) created from viewpoints placed on the lowest points

	TIN						**DEM**					
	highest		**lowest**		**random**		**highest**		**lowest**		**random**	
	single	multi	single	multi	single	multi	single	multi	single	multi	single	multi
Prick	0.75	0.97	0.41	0.83	0.64	0.93	0.63	0.90	0.10	0.19	0.18	0.64
TRI	0.44	0.58	0.62	0.72	0.61	0.63	-0.52	-0.38	-0.27	-0.30	-0.34	-0.43
TSI	0.45	0.69	0.69	0.81	0.63	0.75	-0.53	-0.40	-0.24	-0.23	-0.32	-0.42
FD	-0.56	-0.73	-0.64	-0.78	-0.66	-0.76	0.11	-0.27	0.27	0.25	0.27	-0.01

Table 1. The correlation coefficients (*R* values) between the attributes and viewshed complexity

Source code available from https://github.com/GTMeijer/TIN_Viewsheds.

cover valleys), and picking viewpoints uniformly at random. To avoid clusters of high or low viewpoints we overlay an evenly spaced grid on the terrain, and pick one viewpoint from every grid cell (either the highest, lowest, or a random one). We pick these points based on the DEM representation of the terrains, and place the actual viewpoints one meter above the terrain to avoid degeneracies. We use the same locations in the TINs in order to compare the results between TINs and DEMs (we do recompute the z-coordinates of these points so that they remain 1m above the surface of the TIN). The resulting viewsheds follow the expected pattern; refer to Figure 7. In our experiments, we consider both the complexity of a viewshed of a single viewpoint as well as the combined complexity of a viewshed of nine viewpoints (picked from a 3×3 overlay grid). Results of Kammer et al. [12] suggest that for the size of terrains considered these viewpoints already cover a significant portion of the terrain, and hence picking even more viewpoints is not likely to be informative.

Analysis. For each topographic attribute we consider its value in relation to the complexity of the viewsheds. In addition, we test if there is a correlation between the viewshed complexity and the attribute in question. We compute their sample correlation coefficient (Pearson correlation coefficient) R to measure their (linear) correlation. The resulting value is in the interval [“1, 1], where a value of 1 implies that a linear increase in the attribute value corresponds to a linear increase in the viewshed complexity. A value of “1 would indicate that a linear increase in the attribute leads to a linear decrease in viewshed complexity, and values close to zero indicate that there is no linear correlation.

6. Results

We start by investigating the prickliness values compared to the complexity of the terrains considered. These results are shown in Figure 8. We can see that the prickliness is generally much smaller than the number of vertices in the (TIN representation of the) terrain. In Figure 9 we also see one the $\pi_{\vec{v}}$ values for orientation vectors near (0, 0, 1) (recall that the maximum over all orientations defines the prickliness).

6.1. Topographic Attributes and Viewshed Complexity

For each of the terrains we compute the viewshed of one or nine viewpoints, for three viewpoint placement strategies, and analyze the complexity of the viewshed as a function of the topographic attributes both for TINs and DEMs. Table 1 summarizes the correlation between the attributes and the viewshed complexity for each case.

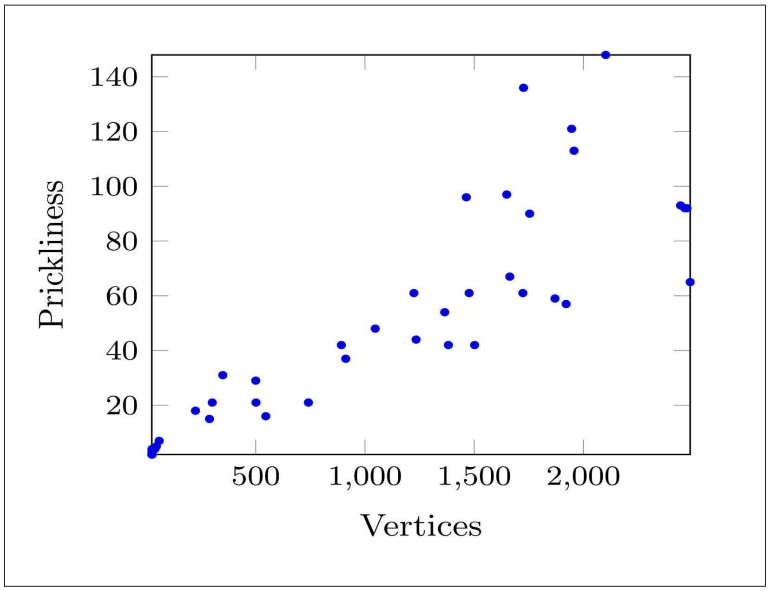

Figure 8. The prickliness values for the terrains we considered

Single Viewpoint. The first row in Figure 10 shows the full results for a randomly placed viewpoint on the TIN. Somewhat surprisingly, we see that terrains with high fractal dimension have a low viewshed complexity. For the other measures, higher values tend to correspond to higher viewshed complexities. However, the scatter plots for these two measures show a large variation. The scatter plots for the other placement strategies (highest and lowest) look somewhat similar, hence the strategy

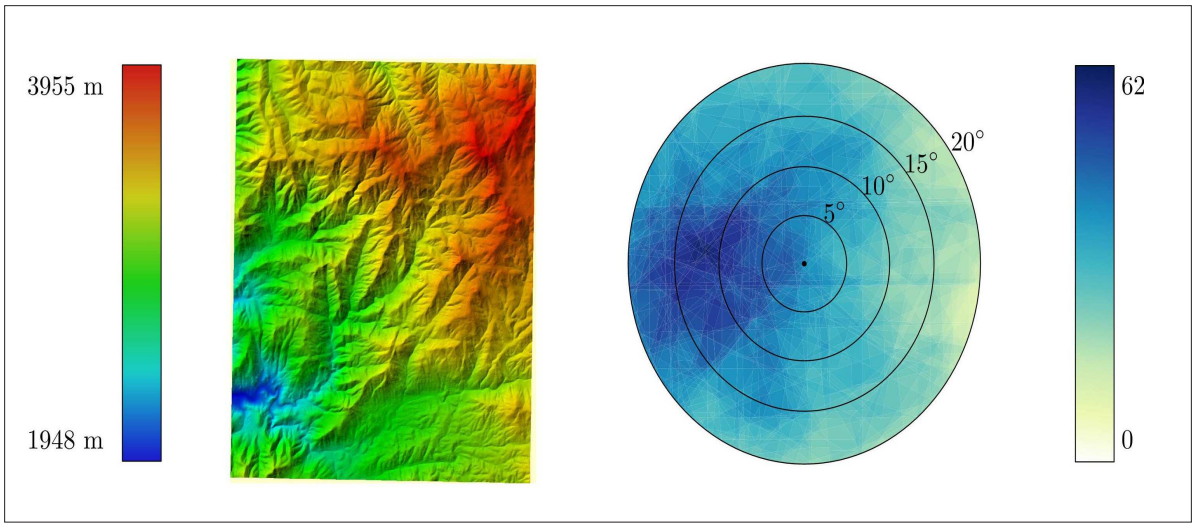

Figure 9. (left) A real-world terrain with 583 vertices from the neighborhood of California Hot Springs whose prickliness is only 62. (right) The value $\pi_{\vec{v}}$ for vectors near $(0,\ 0,\ 1)$

with which we select the viewpoints does not seem to have much influence in this case. None of the four attributes shows a strong correlation in this case (see also Table 1). Prickliness shows weak-medium correlation in three out of six cases, strong correlation for one case – viewpoints at highest points – and no correlation for two cases with viewpoints at lowest points. The other attributes show an even weaker correlation in general.

Multiple viewpoints. The results comparing the topographic attributes to the complexity of the common viewshed of multiple viewpoints, selected from a 3 × 3 overlay grid (refer to Section 5) can be found in the second row of Figure 10. Again, fractal dimension shows an inverse behavior. In contrast, the other three attributes show now a much clearer positive correlation with viewshed complexity. In this case the prickliness shows the strongest correlation in all but one case (that of viewpoints at lowest points). In particular when placing the viewpoints on highest points within the overlay grids the correlation is strong. See also Figure 11 (left).

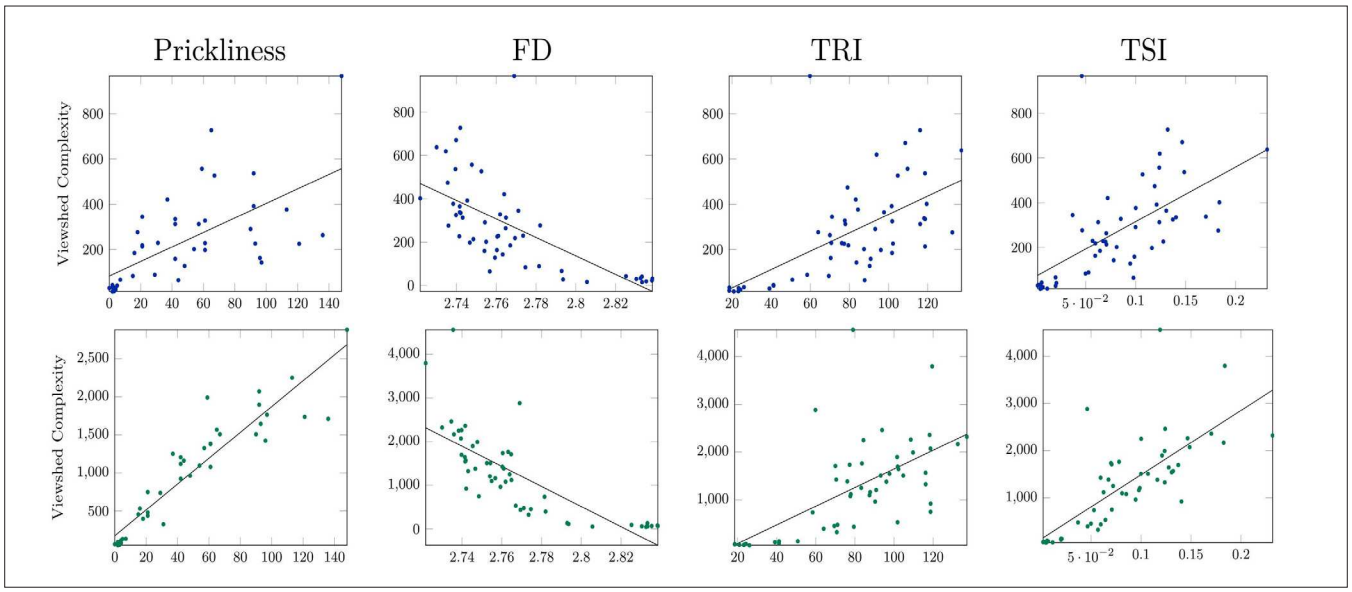

Figure 10. The viewshed complexity on a TIN. First row: single random viewpoint. Second row: common viewshed of multiple (nine, selected from a 3 × 3 overlay) random viewpoints

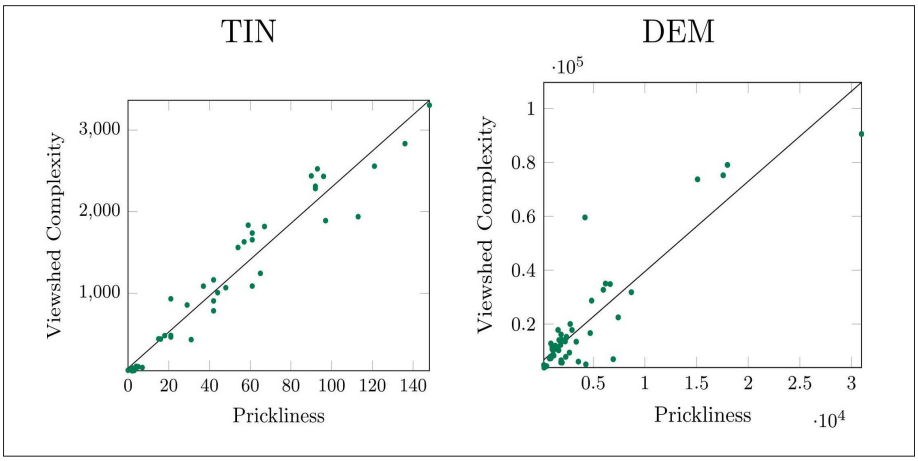

Figure 11. The complexity of the common viewshed of nine viewpoints placed using the highest strategy on a TIN (left) or on a DEM (right)

DEM Results. The scatter plots for randomly placed viewpoints can be found in Figure 12. The first row again corresponds to the complexity of a single viewshed, whereas the second row corresponds to the complexity of the common viewshed of nine viewpoints selected from a 3 × 3 overlay. In contrast to TINs, for DEMs all measures show no to weak correlation values. The correlation between prickliness and the viewshed complexity is the highest with a positive correlation value of 0.629. However, the scatter plot (Figure 11 right) suggests that this value is not very meaningful.

Something similar occurs in the case of viewsheds of DEMs for multiple viewpoints, where none of the measures seems to have a statistical significance, with most of the R^2 values being below 0.200. The exception to this is the correlation between prickliness for viewpoints on highest points, which shows a very strong relationship.

7. Discussion

The experimental results for TINs confirm our hypotheses. We can see a clear correlation between the viewshed complexity and the prickliness, especially when multiple viewpoints are placed on the highest points. In contrast, this is not evident for the other three topographic attributes considered. The terrain ruggedness index (TRI) and terrain shape index (TSI) show some very weak positive correlation, but not as strong as prickliness. This could be explained by the fact that TRI and TSI only consider a fixed neighborhood around each point, making them local measures unable to capture the whole view shed

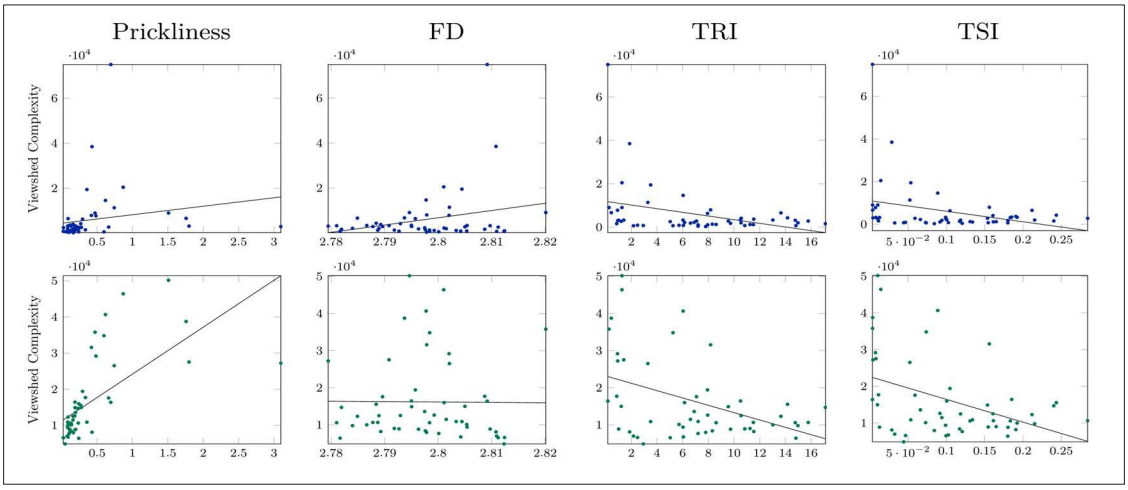

Figure 12. The viewshed complexity on a DEM. First row: single random viewpoint. Second row: common viewshed of multiple (nine, selected from a 3 × 3 overlay) random viewpoints. The prickliness values are times 104

complexity. Indeed, a small (local) obstruction can be enough to significantly alter the value for any of these attributes. The fractal dimension (FD) seems to be even worse at predicting viewshed complexity. Unlike TRI and TSI, this topographic attribute considers the variability within an area of the terrain as opposed to a fixed-radius neighborhood. Taking a closer look at the FD values for both terrain datasets shows a minimal variation, with most of them being close to 3.0, which, according to Taud et al. [22], indicates a nearly-constant terrain. These results seem to indicate that this measure fails to detect the variation in elevation levels with the chosen parameters.

The situation for DEM terrains is less clear. Only for viewsheds originating from the highest points we see a strong correlation between prickliness and viewshed complexity. When the viewpoints are placed at the lowest points of the DEM terrains, the correlation disappears. Since the prickliness measures the amount of peaks in the terrain in all possible (positive) directions, this means that when a viewpoint is placed at the highest elevation and the viewshed gets split up by the protrusions (which seem to be accurately tracked by prickliness), there is a strong correlation. However, when the viewpoints are placed at the lowest points, the viewsheds become severely limited by the topography of the terrain surrounding them. Even when placing multiple viewpoints, these viewsheds do not seem to encounter enough of the protrusions that are detected by the prickliness measure for viewpoints placed at high points.

One possible explanation for the difference between the results on the TIN and DEM terrains for prickliness could be attributed to the difference in resolution between the DEMs and TINs used. The DEMs used consisted of 1.68M cells of 10m size, while the TINs – generated with an error tolerance of 50m – had 1547 vertices on average. While it would have been interesting to use a higher resolution TIN, this was not possible due to the high memory usage of the prickliness algorithm. Another possible explanation for the mismatch between the results for TINs and DEMs may be on the actual definition of prickliness, which is more natural for TINs than for DEMs. Indeed, it can be seen in the results that the prickliness values for DEMs are much higher than for TINs, which could indicate that the definition is too sensitive to small terrain irregularities.

8. Conclusion

We established that prickliness is a reasonable measure of potentially high viewshed complexity, at least for TINs, confirming our theoretical results. Moreover, prickliness shows a much clearer correlation with viewshed complexity that the three other terrain attributes considered.

One aspect worth further investigation is its correlation for DEMs, which seems to be much weaker. One explanation for this might be that the definition of prickliness is more natural for TINs than for DEMs, but there are several other possible explanations, and it would be interesting future work to delve further into this phenomenon. Having established that prickliness can be a useful terrain attribute, it remains to improve its computation time, so it can be applied to larger terrains in practice.

Finally, during our work we noticed that several of the terrain attributes are defined locally, and are parameterized by some neighborhood size. Following previous work, we aggregated these local measures into a global measure by averaging the measurements. It may be worthwhile to investigate different aggregation methods as well. This also leads to a more general open question on how to "best" transform a local terrain measurement into a global one.

References

[1] Chamberlain, Brent C., Meitner, Michael J. (2013). A route-based visibility analysis for landscape management. *Landscape and Urban Planning*, 111:13–24.

[2] Danese, Maria., Nolè, Gabriele., Murgante, Beniamino. (2011). Identifying viewshed: New approaches to visual impact assessment. *In Geocomputation, Sustainability and Environmental Planning*, pages 73–89. Springer, 2011.

[3] Berg, Mark de., Haverkort, Herman., Tsirogiannis, Constantinos P. (2009). Visibility maps of realistic terrains have linear smoothed complexity. *In: Proceedings of the Twenty-Fifth Annual Symposium on Computational Geometry*, pages 163–168. ACM.

[4] Dean, D. J. (1997). Improving the accuracy of forest viewsheds using triangulated networks and the visual permeability method. *Canadian Journal of Forest Research*, 27 (7) 969–977.

[5] Dong, Youfu., Tang, Guoan., Zhang, Ting. (2008). A Systematic Classification Research of Topographic Descriptive Attribute in Digital Terrain Analysis. *The International Archives of the Photogrammetry, Remote Sensing and Spatial Information Sciences*, 37 B2:357–362, 2008.

[6] Edelsbrunner, Herbert., Guibas, Leonidas J. (1989). Topologically sweeping an arrangement. *Journal of Computer and System Sciences*, 38 (1), 165–194.

[7] Environmental Systems Research Institute (ESRI). Arcgis pro (2.5.1), May 2020.

[8] Environmental Systems Research Institute (ESRI). Terrain, scale: 10m, February 2020.

[9] Franklin, W. Randolph., Vogt, Christian. (2004). Multiple observer siting on terrain with intervisibility or lo-res data. In XXth Congress, *International Society for Photogrammetry and Remote Sensing*, pages 12–23.

[10] Michael, T. Goodrich. (1992). A polygonal approach to hidden-line and hidden-surface elimination. CVGIP: *Graphical Models and Image Processing*, 54 (1) 1–12, January.

[11] Hurtado, Ferran., Löffler, Maarten., Matos, Inês., Sacristán, Vera., Saumell, Maria., Silveira, Rodrigo I., Staals, Frank. (2014). Terrain visibility with multiple viewpoints. *International Journal of Computational Geometry & Applications*, 24 (04), 275–306.

[12] Kammer, Frank., Löffler, Maarten., Mutser, Paul., Staals, Frank. (2014). Practical approaches to partially guarding a polyhedral terrain. *In: Proceedings 8th International Conference on Geographic Information Science*, LNCS 8728, pages 318–332.

[13] Kim, Young-Hoon., Rana, Sanjay., Wise, Steve. (2004). Exploring multiple viewshed analysis using terrain features and optimisation techniques. *Computers & Geosciences*, 30 (9), 1019–1032.

[14] Mandelbrot, Benoit B. (1982). The fractal geometry of nature. W.H. Freeman, New York.

[15] Maynard, J. J., Johnson. M. G. (2014). Scale-dependency of LiDAR derived terrain attributes in quantitative soil-landscape modeling: Effects of grid resolution vs. neighborhood extent. Geoderma, 230-231:29–40.

[16] Henry McNab, W. (1989). Terrain shape index: Quantifying effect of minor landforms on tree height. Forest Science, 35:91–104, 1989.

[17] Meijer, Gert. (2020). Realistic terrain features and the complexity of joint viewsheds. Master's thesis, Utrecht University, 2020.

[18] Moet, Esther. (2008). Marc van Kreveld, and A. Frank van der Stappen. On realistic terrains. Computational Geometry, 41 (1):48–67.

[19] Riggs, Philip D., Dean, Denis J. (2007). An investigation into the causes of errors and inconsistencies in predicted viewsheds. Transactions in GIS, 11 (2) 175–196.

[20] Riley, Shawn J., DeGloria, Stephen D., Elliot, Robert. (1999). A terrain ruggedness index that quantifies topographic heterogeneity. *Journal of Science*, 5:23–27.

[21] Schirpke, Uta., Tasser, Erich., Tappeiner, Ulrike. (2013). Predicting scenic beauty of mountain regions. Landscape Urban Plan., 111:1–12.

[22] Taud, Hind., Parrot. Jean-François. (2005). Measurement of DEM roughness using the local fractal dimension. *Géomorphologie: relief, processus, environnement*, 11 (4) 327–338

[23] The CGAL Project. CGAL User and Reference Manual. CGAL Editorial Board, 5.0.2 edition, 2020.

[24] Wein, Ron., Berberich, Eric., Fogel, Efi., Halperin, Dan., Hemmer, Michael., Salzman, Oren., Zukerman, Baruch. (2020). 2D arrangements. In CGAL User and Reference Manual. CGAL Editorial Board, 5.0.2 edition.

[25] Zhang, Weihua.,Montgomery. (1994). Digital elevation model grid size, landscape representation, and hydrologic simulations. *Water Resources Research*, 30 (4) 1019–1028.